Chapter 10
MRI Appearance of Invasive Breast Cancer

Lea Gilliland and Maria Piraner

Abstract This chapter reviews invasive cancers using both the molecular classification of subtypes of breast cancer and the traditional pathologic classification of breast cancers. MRI is a frequently used modality for evaluating breast cancer. Tumors demonstrate varying morphologic and enhancement characteristics depending on tumor type. Knowledge of the MRI appearance of various tumors is helpful for expanding the differential diagnosis.

Keywords Luminal A/Luminal B breast cancer • Her2 enriched breast cancer • Triple negative breast cancer • Invasive ductal carcinoma • Invasive lobular carcinoma • Papillary carcinoma • Micropapillary carcinoma • Mucinous carcinoma • Medullary carcinoma • Tubular cancer • Metaplastic carcinoma • Adenoid cystic carcinoma • Phyllodes tumor

10.1 Introduction

Dynamic contrast enhanced Breast MRI emerged in the 1990s as a novel technique to detect breast cancer. Its high sensitivity is based on tumor angiogenesis and neovascularity [1]. A 2008 meta-analysis of 44 studies demonstrated that MRI has a sensitivity of 90 % and a specificity of 72 % [2]. A 2007 prospective study of 171 patients in a high risk population reported that MRI detected 100 % of the cancers while mammography identified 33 % of cancers and ultrasound demonstrated 17 % [3]. Whereas mammography uses x-rays and ultrasound uses sound waves, MRI employs a powerful magnetic field, radiofrequency pulses, and high soft tissue contrast to capture tumor morphology.

L. Gilliland, MD (✉)
Department of Radiology, Emory University Hospital, Atlanta, GA, USA
e-mail: lcgilli@emory.edu

M. Piraner, MD
Department of Radiology and Imaging Sciences, Emory University Hospital, Atlanta, GA, USA

S.L. Heller, L. Moy (eds.), *Breast Oncology: Techniques, Indications, and Interpretation*, DOI 10.1007/978-3-319-42563-4_10

10.2 Categorization of Invasive Breast Disease

Invasive breast cancers may be categorized in a variety of ways. This chapter will review the molecular and histopathologic classification of types of invasive breast tumors and discuss morphologic and kinetic appearance of invasive breast disease on MRI. Although this chapter will focus predominantly on the MRI phenotypic appearance of invasive cancers, it is important to recognize that more recently, molecular classifications have been identified.

10.3 Molecular Classification

To determine the molecular signature of breast cancer, messenger RNA is isolated and tested against complementary DNA microarrays to determine which genes a cancer expresses, and which genes it lacks [4]. It has been noted that breast cancers can be divided into two large categories, depending on the pattern of gene expression. When tumor cells have characteristics similar to the epithelial cells lining the milk ducts, expressing cytokeratin 8/18 and genes associated with the estrogen receptor (ER), the cancers are labeled luminal cancers [4]. Alternatively, when cancer cells display characteristics similar to the myoepithelial cells (also known as basal cells) that line the inner surface of the basement membranes, expressing cytokeratin 5/6 and laminin, the cancers are grouped into the basal category [4]. These two large categories of luminal breast cancers and basal breast cancers are defined and classified on the basis of the presence or absence of ERs [4] which defines the morphology and behavior of a tumor. Luminal tumors also are characterized by an absence of overexpression of the gene ERBB2 (also known as the HER2/neu gene), a proto-oncogene that stimulates cellular growth [4].

Other markers of cell proliferation and invasiveness have been analyzed over the past decade and four subgroups of breast cancer have been adopted. These are luminal A, luminal B, HER2-enriched, and basal-like cancers. Luminal A breast cancers express both estrogen (ER) and progesterone (PR) receptors and are generally low grade. HER2/neu is not amplified and there is a low Ki-67 proliferative index. This is the most common type of breast cancer, representing 50 % of all breast cancers. 5-year survival is greater than 80 % [4]. Luminal B cancers also express ER and PR but have higher Ki-67 levels and, thus, greater proliferative activity. Luminal B cancers generally do not overexpress HER2/neu, but 30 % will be Her2-enriched [4]. Five-year survival is 40 %. HER2-enriched tumors have extra copies of the HER-2 gene and over produce a growth enhancing protein ERBB2. This results in increased cellular aggressiveness and fast growth. Sixty-six percent of HER2- enriched cancers overexpress HER2/neu and the remaining tumors express overexpress genes in the *ras* pathway [4] 30–40 % HER2- enriched cancers are ER and PR positive. Basal like subtypes lack ER, PR, and HER2/neu markers and overexpress oncogenes that favor cell proliferation and carcinogenesis such as

p53. Eighty percent of triple negative breast cancers are basal-like. Basal-like cancer is more common in younger BRCA1 carriers and in young African American women [4]. Specific imaging findings can be seen in Luminal A, Luminal B, Her2-enriched, and basal type cancers.

10.3.1 Luminal A/Luminal B

Luminal A and Luminal B are grouped as ER+ HER2- cancers for imaging purposes. Mammographically, these cancers often present as masses; calcifications are seen in 41 % of these cancers. Ultrasound often demonstrates irregular masses with angular or microlobulated margins [4]. 117 ER-positive HER2- negative breast cancers were studied by Uematsu and colleagues and MRI findings were reported as 67 % mass enhancement and 33 % nonmass enhancement (NME). Masses were irregular (32 %) and oval in shape (38 %) with irregular margins (86 %) (Fig. 10.1). Heterogeneous internal enhancement was seen 97 % of the time with kinetics being plateau or washout in 79 % of cases. Lesions were iso- to hypointense on T2-weighted images 85 % of the time [5].

10.3.2 Her2 Enriched

Although Her 2 positive tumors are not a perfect correlate for the HER2 enriched subtype, 60 % of HER-2 positive tumors are HER-2 enriched tumors. MRI features of HER2-positive tumors have been documented. HER-2 positive tumors have been reported to present as masses with microcalcifications [4]. Calcifications have been noted in as many as 78 % of HER2-positive tumors [4]. HER-2 cancers are often associated with DCIS, more than other breast cancer subtypes. Youk and colleagues reported MR characteristics of 94 HER2-positive cancers: mass enhancement was noted in 90 %; 47 % of masses were round or oval and 41 % were lobulated. Margins were spiculated (51 %) and irregular (48 %). Heterogeneous enhancement was most commonly seen (79 %) and washout was the most common kinetic pattern (90 %) Her-2-positive cancers demonstrate non-mass enhancement more often than the other subtypes [4] (Fig. 10.2).

10.3.3 Triple Negative/Basal

MRI characteristics reflect histology in triple negative cancers/basal-like breast cancers [5–6]. Triple negative breast cancer (TNBC) refers to invasive cancers that lack estrogen receptors (ER negative), progesterone receptors (PR negative), and are human epidermal growth factor receptor negative (HER2 negative). The majority of TNBCs are basal like. TNBCs are associated with the BRCA1 mutation and early metastatic

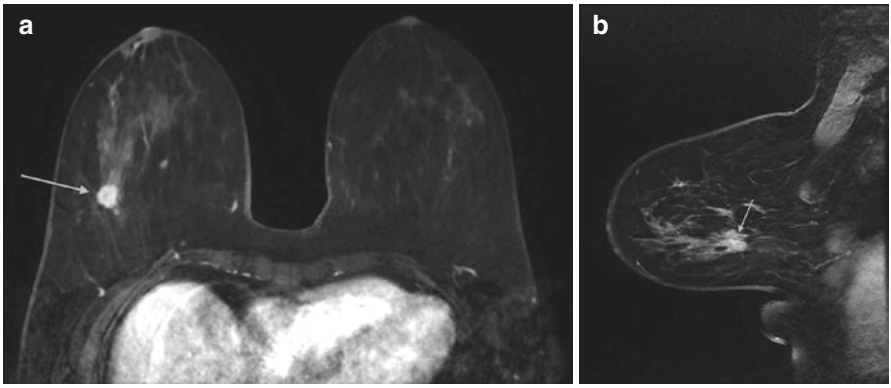

Fig. 10.1 Axial and sagittal T1 post contrast images demonstrate an irregularly shaped and irregularly marginated mass with heterogeneous enhancement (*arrows*). Biopsy demonstrated ER/PR + HER-2- IDC

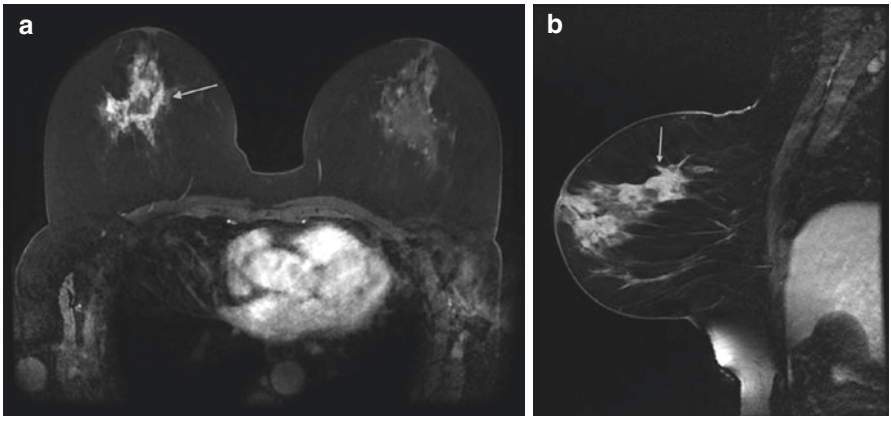

Fig. 10.2 Axial and Sagittal T1 post contrast images demonstrate an irregular mass with associated nonmass enhancement (*arrow*). Biopsy revealed HER2+ IDC

disease [6]. Clinically, this denotes a poor prognosis because tumors that are ER/PR negative do not respond to hormonal therapy. Also, targeted therapy with monoclonal antibodies against HER 2 will not work in tumors that are HER2 negative. TNBCs are typically high-grade [5]. Histologically, triple negative breast cancers are associated with the presence of a central scar, tumor necrosis, the presence of spindle cells or squamous metaplasia, high total mitotic count, and high nuclear-cytoplasmic ratio [5].

TNBCs often appear as circumscribed round or oval masses and are less likely to show distortion or calcifications [7]. Ultrasound frequently demonstrates a solid hypoechoic or mixed echogenicity oval, round or irregular mass with circumscribed or indistinct margins [5, 8]. TNBCs are generally seen as mass lesions on MRI with very few appearing as non-mass enhancement (NME) (Fig. 10.3). Masses may be round, oval or irregular with circumscribed, irregular or spiculated margins. Differentiation from benign masses can be difficult, as many features such as oval,

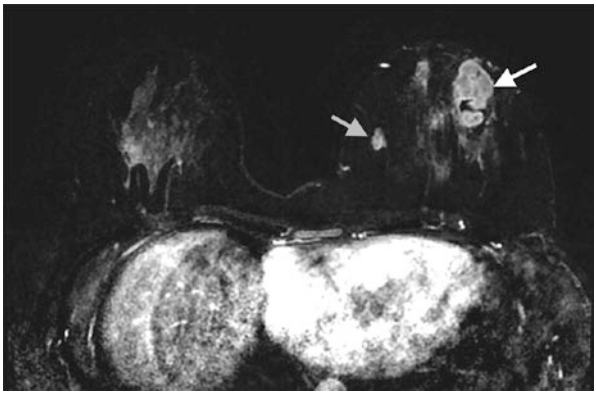

Fig. 10.3 Axial T1-weighted post contrast subtraction image demonstrates an irregularly shaped circumscribed mass with heterogeneous enhancement (*white arrow*). A smaller similar mass is noted medially (*gray arrow*). Biopsy of the large and small masses yielded triple negative cancer

circumscribed masses, persistent enhancement, and high T2 signal are seen both in benign lesions and TNBCs, although the high T2 signal in a TNBCs is often due to necrosis (Fig. 10.3). Rim-enhancement and internal, enhancing septations should increase suspicion if seen [7]. TNBCs are more likely than other cancers to have persistent enhancement kinetics [7].

10.4 MRI Tools for Detecting Invasive Cancer

10.4.1 MR-BI-RADS and Descriptors of Invasive Carcinomas

The MR-BI-RADS lexicon identifies specific morphologic and kinetic characteristics for Enhancing lesions and is discussed in Chap. 2, so will only briefly be addressed here. The combination of morphologic and kinetic features has a reported sensitivity of 90 % and a specificity of 72 % for detecting malignancy [2].

10.4.1.1 Morphologic Features of Invasive Disease

Invasive cancer may present as a mass, NME or a focus on MRI. A 2007 study reviewed MRI biopsy results found the probability of malignancy to be 34 % for masses, 27 % for NME, and 19 % for foci [9]. Certain lesion characteristics should raise suspicion for malignancy and invasive disease, in particular masses with irregular and spiculated margins [10, 11]. A 2006 study documenting the characteristics of 171 masses on MRI demonstrated the most frequent morphological finding in malignant lesions was heterogeneous internal enhancement (96 % of malignancies demonstrated in the delayed phase and 90 % in the early phase). Features with the highest positive predictive value for carcinoma were spiculated margin (100 %), delayed central enhancement (100 %), enhancing internal septations in the delayed phase (97 %), and irregular shape (97 %). Of the masses studied 25 % of smooth round or oval masses were malignant, 85 % of irregularly-shaped or marginated

masses were malignant and 100 % of spiculated masses were malignant. Smooth margins were the most frequent finding in benign lesions (80 %) [11]. Regarding masses, a 2012 study of 969 patients demonstrated the highest PPV was found with irregular margins (PPV, 0.196) and spiculated margins, (PPV, 0.333). The lowest PPV was found with smooth margins (PPV, 0.052). Masses with marked internal enhancement were most likely to represent cancer (PPV, 0.231). Both plateau (PPV 0.152) and washout (PPV, 0.178) were associated with cancer [12].

10.4.1.2 Kinetic Features of Invasive Disease

Tumor enhancement may be plotted on a time-signal intensity curve. The initial contrast enhancement and the delayed contrast enhancement characteristics are calculated. These kinetic curves have become a standard component of the breast MRI exam and allow for better prediction of malignancy. Due to angiogenesis, malignancies demonstrate rapid wash-in and wash-out of the contrast agent. This is known as a type 3 time-signal intensity curve. This type 3 pattern is the most concerning curve type. However, benign entities (such as lymph nodes) may demonstrate this washout curve. In addition, a persistent or plateau curve may be seen in both benign and malignant lesions [10, 13]. A 2010 study comprised of 120 malignancies, both in situ and invasive cancers, demonstrated persistent enhancement in 10 % of masses, plateau enhancement in 48.6 %, and washout in 41 % of masses [13]. Enhancement patterns of NME were less specific for malignancy [13].

10.4.2 Evolving MRI Techniques for Imaging Invasive Disease

10.4.2.1 Diffusion Weighted Imaging

New functional MRI tools may improve the sensitivity of MRI for detecting invasive disease. Diffusion weighted imaging (DWI) is one such technology (Fig. 10.4) and is discussed in detail in Chap. 15. Malignant breast tumors have high cellularity and often demonstrate restricted water diffusion (high signal intensity) and lower apparent diffusion coefficient (Fig. 10.4). Studies demonstrate an increase in specificity compared to contrast-enhanced MRI alone [14]. A 2010 study of 84 breast lesions demonstrated 97.9 % sensitivity and 75.7 % specificity of DWI. The addition of DWI to standard MRI may be particularly helpful in increasing MRI specificity for malignancy, with one study demonstrating a 13.5 % increase in specificity [15].

10.4.2.2 MR Proton Spectroscopy

Proton MR spectroscopy (1H-MRS) is discussed in detail in Chap. 15. Spectroscopy may be used to help characterize lesions. The choline concentrations in tumors may be associated with increased membrane synthesis by replicating cells and therefore

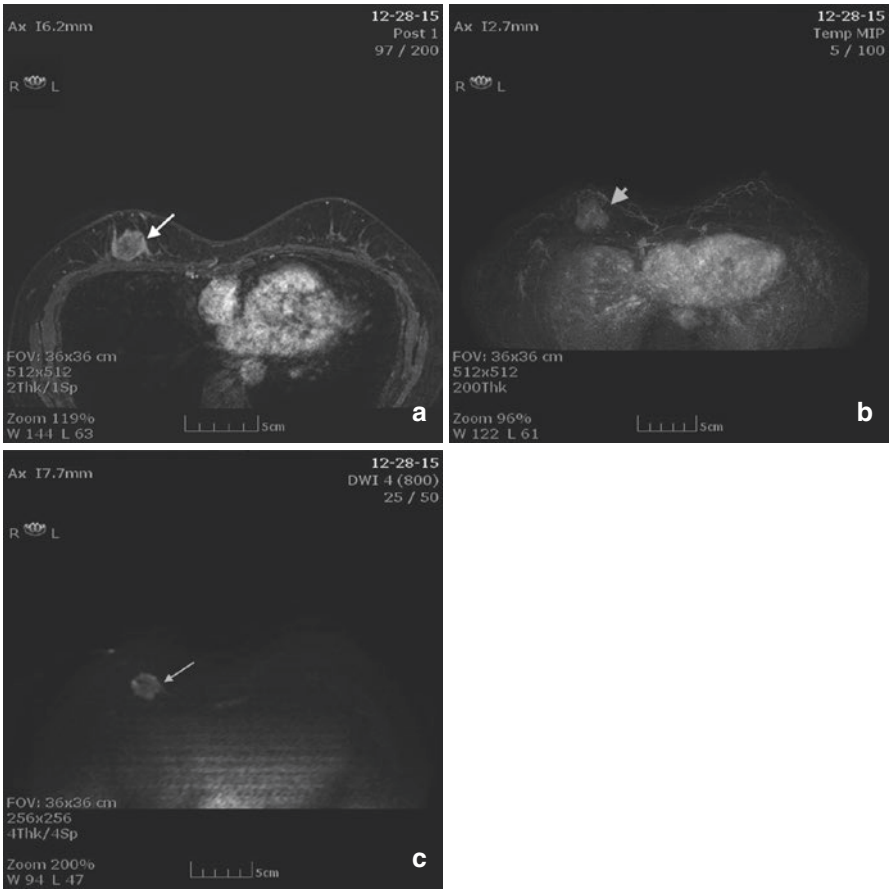

Fig. 10.4 (**a**) Axial T1 post contrast image demonstrates a round rim enhancing mass with an irregular border (*arrow*). (**b**) MIP image demonstrates enhancement within the mass (*arrowhead*). (**c**) DWI image demonstrates bright signal within the mass indicating restricted diffusion (*arrow*)

with biologic aggressiveness [16]. Increased total choline-containing compound has been associated with overexpression of the HER-2neu gene [17] and with an aggressive breast cancer phenotype [17, 18]. Studies show that tCho detection rate is higher in invasive cancer compared to DCIS, possibly associated with more aggressive behavior and/or faster cell replication.

Choline kinase overexpression has been found to be significantly associated with high histologic grade and ER-negative status [16]. These associations may be due to increased cell proliferation. ER is considered a favorable prognostic indicator in breast tumors as ER-positive tumors are more likely to be well differentiated and less aggressive. Patients with ER-positive tumors have more therapeutic options, such as ER blockers or aromatase inhibitors, than do patients with ER-negative tumors. A study of ER status and MR spectroscopic features found that the total choline-containing compound detection rate was higher in ER-negative patients [16].

HER-2/neu is associated with an aggressive tumor phenotype and reduced survival rate. The intracellular domain of HER-2 neu has tyrosine kinase activity that regulates cell growth and proliferation [19]. HER-2 neu is overexpressed in 20–25 % of invasive breast cancers and has been associated with more aggressive tumors, early relapse, and shorter survival [20]. The choline detection rate has been found to be higher in HER-2 neu- positive than in HER-2 neu-negative tumors. Additionally, triple-negative tumors showed significantly higher signal-to-noise ratio (SNR) than did non–triple-negative tumors [20]. Shin and colleagues found that on MRS, IDCs were consistently positive for choline whereas DCIS and IDC with an extensive intraductal component (EIC) were likely negative [18]. SNR was significantly higher in tumors of high histologic grade than lower histologic grade [18]. In summary, proton MRS may be an imaging biomarker for malignancy.

10.5 Radiologic-Pathologic Correlation and Invasive Disease

10.5.1 Specific Tumor Types and MRI Appearance

Traditional pathologic classification divides invasive disease into two major subtypes: invasive ductal carcinoma and invasive lobular carcinoma. Invasive ductal carcinoma not otherwise specified (IDC-NOS) is the most common. The remaining ductal cancers are further subdivided into unusual ductal carcinomas including papillary, micropapillary, mucinous, tubular, and adenoid cystic. Stromal malignancies including metaplastic carcinomas, phyllodes, and sarcomas are rarely encountered. MRI appearance varies according to histologic type; however, tremendous overlap is present.

10.5.2 Invasive Ductal Carcinoma NOS

IDC NOS comprises 85 % of breast cancers. The presence of glandular differentiation and intercellular cohesion defines ductal differentiation. However, most ductal carcinomas consist of invasive tubules and glands and have no specific type designation [21]. These tumors often elicit a scirrhous reaction, resulting in the irregular border seen on MRI. However, high-grade ductal carcinomas may grow so rapidly that there is no time for a scirrhous reaction, resulting in circumscribed borders. This circumscribed appearance is more common in BRCA related carcinomas [21].

Common MRI findings are an irregularly-shaped mass with heterogeneous enhancement and irregular or spiculated margins (Fig. 10.5). Also, peripheral or rim enhancement can be seen. Although IDC-NOS is typically not bright on T2 -weighted images, some IDC-NOS demonstrate areas of T2 hyperintensity secondary to necrosis [22]. The margins of lesions are often best characterized on nonfat saturated T1-weighted images. Surrounding breast tissue must be carefully evaluated, as small satellite masses may be present. Satellite lesions are masses with similar enhancement

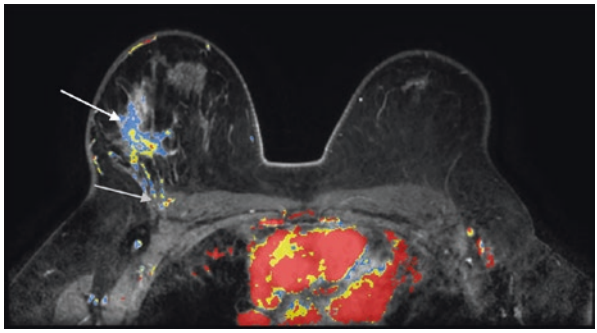

Fig. 10.5 Axial post contrast color image shows an irregular mass with heterogeneous enhancement (*white arrow*). Note the loss of a fat plane between the mass and the pectoralis muscle, as well as enhancement of the pectoralis (*gray arrow*). Biopsy revealed IDC NOS

characteristics as the primary cancer, but are smaller, and usually in close proximity. Contrast enhancement characteristics may vary but the most common pattern is rapid wash-in and rapid wash-out (type 3 curve) [22].

10.5.3 Papillary Carcinoma

10.5.3.1 Histology and Presentation

Papillary carcinoma is a rare variant of invasive ductal carcinoma accounting for less than 2 % of carcinomas and is most commonly found in postmenopausal women [23, 24]. Histologically, the epithelium proliferates into villous-like projections that eventually fill the lumen [23]. Papillary carcinoma is differentiated from a papilloma by the malignant appearing epithelial cells and an absent myoepithelial layer. Papillary carcinomas are subdivided into solid, intracystic without invasion, intracystic with a focus of invasion, and invasive papillary carcinoma [24]. This carcinoma may arise in the central ducts and is located in the retroareolar region in about 50 % of patients [24]. Bloody nipple discharge is present in 22–34 % of patients [23]. Patients with papillary carcinoma often have a better prognosis than patients with IDC-NOS. Axillary lymph nodes are involved less often in patients with papillary carcinoma than in patients with other types of ductal carcinoma [23].

10.5.3.2 Imaging

Papillary carcinomas are frequently round, oval, and circumscribed on mammography [23]. This round appearance is due to their cystic component [25]. Papillary cancers do not produce a fibrotic reaction and generally do not show spiculation by mammography. Ultrasound features are a solid hypoechoic or mixed solid and cystic mass with vascularity [23]. Differentiation from benign papillary lesions can be difficult. MRI features of papillary carcinomas are an irregular or round, enhancing mass, often near the nipple. Papillary carcinomas may be bright on both T1 and T2

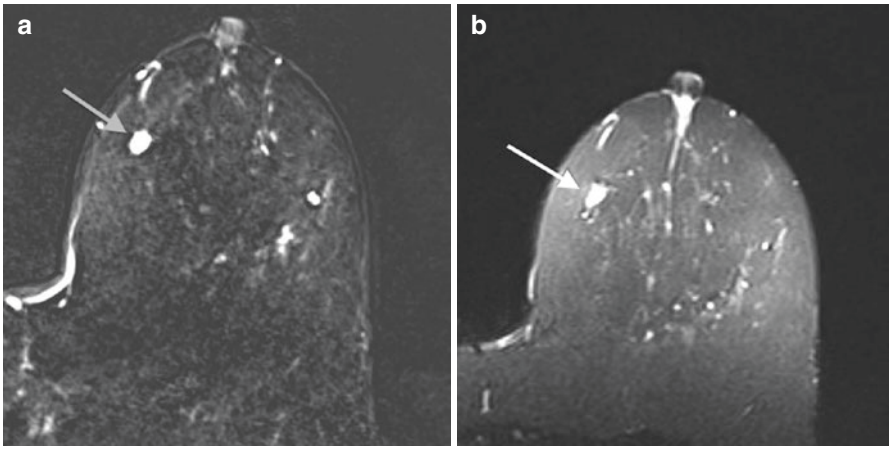

Fig. 10.6 (**a**) Axial T1 post contrast subtraction image demonstrating and oval circumscribed enhancing mass (*gray arrow*). (**b**) Axial T2 image demonstrating increased signal intensity (*white arrow*). Biopsy revealed papillary carcinoma

images. [25]. Intracystic papillary carcinoma will have hyperintensity on T2-weighted images (Fig. 10.6). Enhancement curves can vary from type 1 to type 3. MRI may be helpful in delineating multiple papillary masses [25].

10.5.4 Invasive Micropapillary Carcinoma

10.5.4.1 Histology and Presentation

Invasive micropapillary carcinoma (IMPCa) is a histologic pattern of breast cancer characterized by small, tightly cohesive groups of neoplastic cells disposed within well-delineated clear spaces resembling lymphatic vessels [26]. Micropapillary carcinomas of the breast are described pathologically as having numerous small pseudo-papillary clusters of cells without fibrovascular cores and clusters surrounded by clear spaces [23, 27]. Micropapillary carcinomas account for less than 2 % of breast cancers [23]. They have a worse overall prognosis than IDC-NOS [23]. Various studies report varying percentages of metastatic disease to axillary lymph nodes from 64 to 90 % [27, 28].

10.5.4.2 Imaging

Mammographic appearances include masses displaying a lobulated or irregular shape with spiculated or indistinct margins. Architectural distortion may also be present [23]. When calcifications are associated, they are typically fine pleormorphic or linear branching. Ultrasound features include a hypoechoic or mixed echogenicity mass with irregular shape and spiculated, microlobulated, or indistinct margins.

Fig. 10.7 Axial T1 subtraction image demonstrates an enhancing spiculated mass with spiculated borders (*arrow*). Biopsy revealed invasive micropapillary carcinoma

MRI findings include masses displaying an oval/round or irregular shape with irregular or spiculated margins [29] (Fig. 10.7). Initial rapid enhancement with washout or plateau kinetics in the delayed phase may be observed. Internal enhancement may be homogeneous or heterogeneous [29]. NME has also been reported. Careful attention should be paid to lymph nodes as invasive micropapillary carcinoma has a predilection for lymph node involvement [29].

10.5.5 Medullary Carcinoma

10.5.5.1 Histology and Presentation

Medullary carcinoma of the breast is rare, accounting for less than 5 % of breast cancers [30]. It is defined by the World Health Organization (WHO) classification of breast tumors as "a well-circumscribed carcinoma composed of poorly differentiated cells arranged in large sheets, with no glandular structure, scant stroma, and a prominent lymphoplasmacytic infiltrate" [30]. It is most commonly seen in women in their late 40s and early 50s and has a more favorable prognosis than IDC-NOS [30]. A higher incidence of medullary carcinoma is noted in patients with BRCA1 mutation. A series of 1490 patients managed with breast-conservation therapy that consisted of lumpectomy and radiation therapy at Yale University included 46 cases

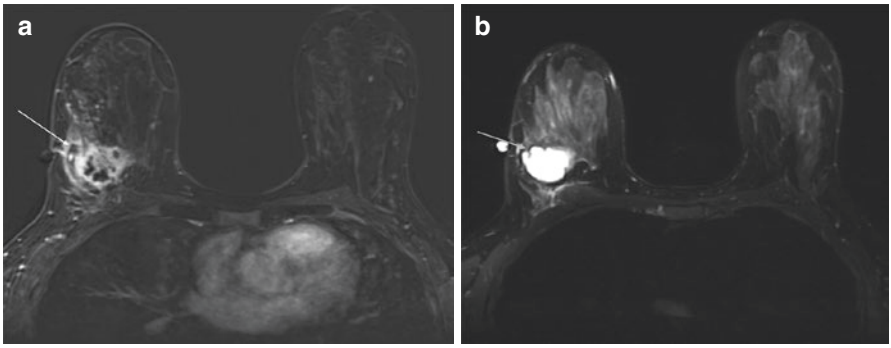

Fig. 10.8 (**a**) Axial T1 post contrast subtraction image demonstrates a mass with an irregular border and rim enhancement characteristic of medullary carcinomas (*white arrow*). (**b**) T2 image demonstrates hyperintense signal within the mass (*gray arrow*). Biopsy revealed medullary carcinoma

of medullary carcinoma. The 10-year distant relapse-free survival in the medullary cohort was significantly better than in the control group of IDC NOS (94.9 % vs. 77.5 %, p = 0.028) [30].

10.5.5.2 Imaging

Mammographic appearance is a dense oval or round mass with circumscribed or microlobulated margins. Ultrasound appearance may be confused with a fibroadenoma [30]. Often medullary carcinomas are circumscribed, hypoechoic, parallel masses with varying degrees of through transmission [30]. The MRI appearance has been reported as isointense on T1-weighted and isointense or slightly hyperintense on fat-saturated T2-weighted images. Medullary carcinomas have oval or round shapes and smooth margins upon contrast enhancement. Heterogeneous enhancement with delayed, peripheral enhancement on late-phase contrast MRI has been reported [30]. Rapid wash-in and rapid wash-out or plateau enhancement is often seen. The peripheral rim enhancement correlates with a peripheral compressed fibrous tissue with prominent lymphocytic infiltration noted at pathology [30] (Fig. 10.8).

10.5.6 Mucinous Carcinoma

10.5.6.1 Histology and Presentation

Mucinous carcinoma, also known as colloid, mucous, or mucoid carcinoma of the breast is a well-differentiated type of invasive adenocarcinoma characterized by large amount of extracellular epithelial mucus. Mucinous carcinoma constitutes

1–7 % of breast carcinomas. Two subtypes of mucinous carcinoma may be differentiated histologically: pure and mixed. The pure type typically has indolent growth, while the mixed type has variable biological behavior, often similar to IDC-NOS. The pure type typically demonstrates a lower histological grade (well-differentiated tumors), higher hormone receptor expression, lower incidence of adverse oncogenes, lower rate of axillary lymph node involvement at diagnosis, and longer disease-free survival [31].

10.5.6.2 Imaging

Mucinous carcinoma may present as circumscribed lesions. A multimodality approach is helpful to reach appropriate diagnosis as well as to differentiate between the two histological types of the neoplasm. Typically, a mucinous carcinoma presents as an oval or round mass with circumscribed margins. At mammography, the pure type correlates with circumscribed or microlobulated margins while the mixed type presents with more indistinct or spiculated contours secondary to a higher degree of fibrosis and peripheral desmoplasia, similar to a IDC-NOS. Microcalcifications are uncommon and may be associated with peripheral component of DCIS [32]. Sonographically, mucinous carcinomas are often heterogeneous in echogenicity and may have mixed solid and cystic components. Posterior acoustic enhancement is common [33].

Mucinous carcinoma on MRI typically has a lobular shape, homogeneous and markedly high signal intensity on T2-weighted images, and a persistent enhancement pattern on dynamic MR images (with rim-like peripheral or heterogeneous internal enhancement). Thus, it has MR imaging features of both benignity and malignancy (Fig. 10.9). The combination of MR imaging features is useful for preoperative diagnosis of the tumor [34]. High signal intensity on T2-weighted images is seen in a pure mucinous carcinoma because the entire tumor is filled by mucin. In mixed mucinous carcinomas, the solid component is identifiable by its relative signal hypointensity on the T2-weighted images [35].

High signal intensity of the mucinous cancer on T2-weighted images is not pathognomonic because other lesions such as necrosis, hemorrhage, edema, myxoid matrix or cystic component are also high signal [36]. On dynamic contrast-enhanced sequences, variable enhancement morphology may occur; however, peripheral, ring-shaped, or heterogeneous enhancement are more characteristic and progressive along time. Enhancing internal separation may also be present. The pure type of mucinous cancer generally demonstrates mild to moderate enhancement at the early phases, with type 1 (persistent) curves or type 2 (plateau) curve. The persistent enhancement pattern is related to the tumor cellularity, nuclear grading, and amount of extracellular mucin. Thus, an intense enhancement in the first 2 min after gadolinium injection, or a type 3 curve (washout) must raise suspicion of mixed-type MMC or, an even rarer pure tumor with high cellularity [37].

Compared with other subtypes of breast cancer, mucinous cancers typically demonstrate low signal intensity on diffusion-weighted images and high apparent

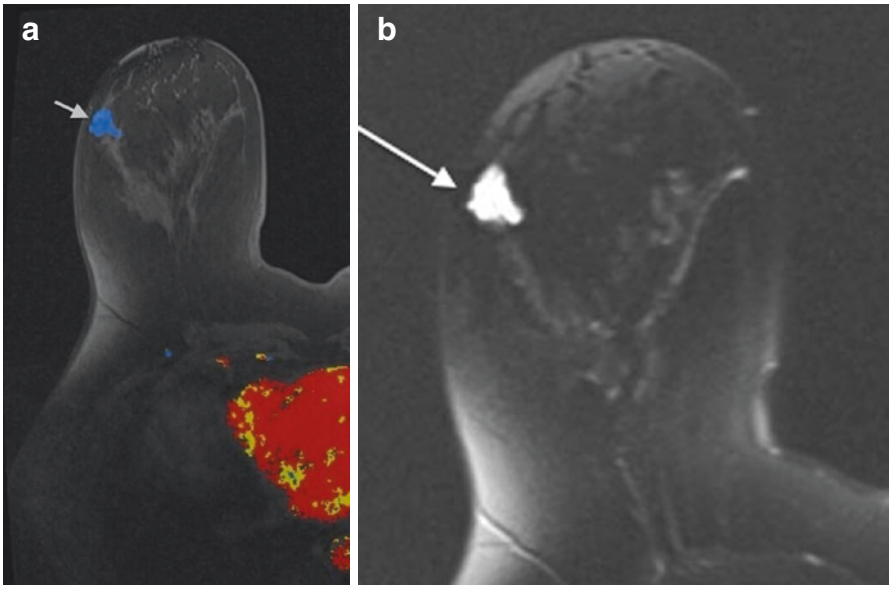

Fig. 10.9 (**a**) Axial T1 post contrast color image demonstrates an irregular mass with plateau (Type II) enhancement (*gray arrow*). (**b**) T2 image demonstrates high signal intensity (*white arrow*). Biopsy revealed mucinous carcinoma

diffusion coefficient (ADC) values in relation to IDC-NOS. High ADC values may be associated with the presence of extracellular mucin and low tumor cellularity.

10.5.7 Tubular Carcinoma

10.5.7.1 Histology and Presentation

Tubular carcinoma of the breast is a sub-type of IDC-NOS. The peak age at presentation is comparatively younger than with other types of breast cancer. Median age at diagnosis is in the mid- to late 40s. Most tubular carcinomas are non-palpable and found incidentally at screening rather than manifesting with clinical findings [38]. Although tubular carcinomas may contain other histologic elements, an excess of 75 % tubular elements is usually required for the diagnosis of tubular carcinoma [38]. A distinguishing pathological feature is a single layer of cells lining tubules with loss of lobular architecture and surrounding infiltration. The glands in tubular carcinomas lack myoepithelial cells. Lesions may be multifocal or multicentric in 10–20 % of cases [39].

Invasive cancers containing tubular elements are not uncommon; however, pure tubular carcinoma is rare and accounts for less than 2 % of all breast cancers. Less pure tubular carcinomas are referred to as mixed tubular carcinomas. A third type is tubulolobular carcinoma has both tubular and infiltrating lobular elements.

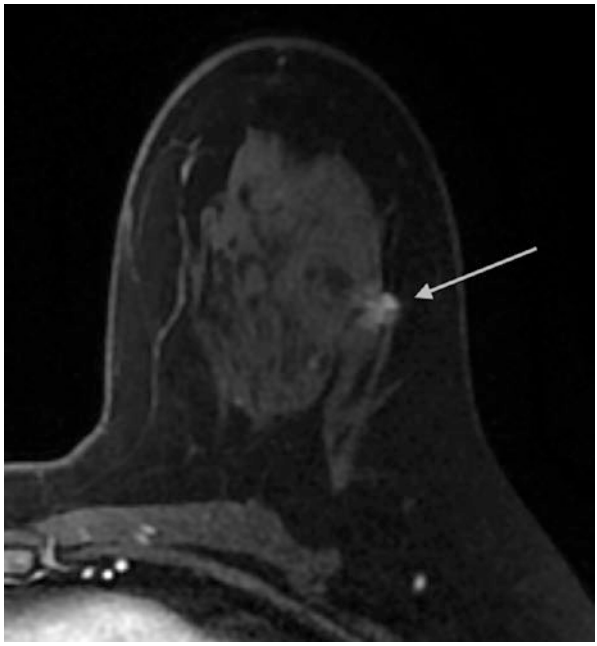

Fig. 10.10 Axial post contrast T1 image demonstrates a small left sided spiculated mass with heterogeneous enhancement (*arrow*). Biopsy revealed tubular carcinoma

10.5.7.2 Imaging

In the majority of cases, on mammography, the lesion is small (< 1 cm), spiculated, and can occur with or without calcifications. The appearance mimics typical IDC-NOS manifesting as one or more small, spiculated masses. The spicules are often longer than the central mass. Amorphous microcalcifications may be present in 10–15 % of cases [39]. On sonography, the appearance also mimics IDC-NOS, presenting as a hypoechoic solid mass with ill-defined margins and posterior acoustic shadowing. Dynamic subtraction MR-imaging might show characteristics of a malignant tumor and cannot be differentiated from IDC-NOS based on MR imaging alone (Fig. 10.10). The prognosis is usually excellent with survival of 97 % at 10 years. The pure tubular forms carry the best prognosis.

10.5.8 Adenoid Cystic Carcinoma

10.5.8.1 Histology and Presentation

Adenoid cystic (ACC) is a rare variant of IDC accounting for 0.1 % of breast cancers [40]. Histologically, ACC is characterized by small basaloid cells with a solid cribriform pattern or tubular growth patterns enclosing pseudoglandular spaces with minimal eosinophilic material [40]. The cell of origin is unknown, but may arise from the ductal epithelium and myoepithelium. Adenoid cystic carcinoma has various growth patterns: glandular, tubular, and solid [40]. Patients typically present with a painful

subareolar palpable mass. Prognosis is excellent with 10 year survival around 98 %, despite being ER/PR negative.

10.5.8.2 Imaging

Mammography demonstrates an ill-defined, lobulated mass with rare calcifications. Ultrasound demonstrates a hypoechoic or mixed ecogenicity mass with irregular borders and minimal color flow [41]. MRI features can include circumscribed or spiculated margins (Fig. 10.11) [41]. Enhancement kinetics have been described from type 1 to type 3. Initial enhancement has been described as rapid and heterogeneous [41]. ACC with primarily solid features may demonstrate high signal on T2-weighted images [41].

10.5.9 Invasive Lobular Carcinoma

10.5.9.1 Histology and Presentation

Invasive lobular carcinoma (ILC) is the second most common histologic type of breast carcinoma, accounting for approximately 10–15 % of all invasive breast cancers. ILC spreads as sheets of a single-cell layer along Cooper's ligaments and other structures in the breast. Typically these tumors show a single-file infiltration of malignant cells through the breast stroma with a relative paucity of desmoplastic response, hemorrhage, necrosis, or calcification [42]. Because of this infiltrative growth pattern, ILC is more difficult to detect at clinical examination and mammography than is IDC [43]. ILC is usually larger at diagnosis than IDC and is often multifocal. [44]. ILC has a higher rate of multiplicity and bilaterality than IDC. Lymph node metastases are less common with ILC than IDC for similar size lesions, so the

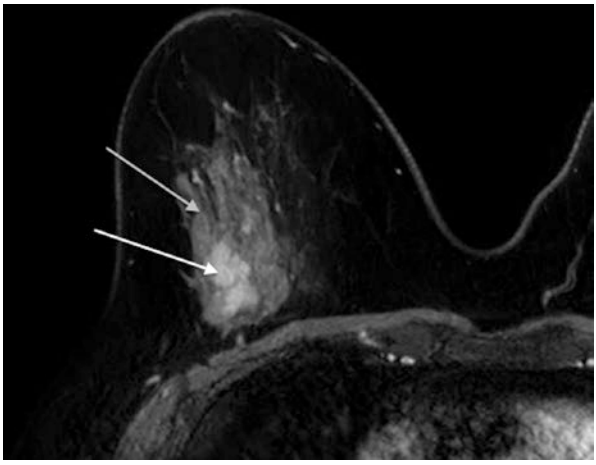

Fig. 10.11 Axial T1 post contrast image demonstrates an irregular heterogeneously enhancing mass. Biopsy revealed adenoid cystic carcinoma. It should be noted that both the central area of intense enhancement (*white arrow*) and the peripheral area of less intense enhancement (*gray arrow*) revealed carcinoma

stage at diagnosis for ILC is overall similar to that for IDC despite the larger size at diagnosis. [44, 45]. However, higher false-negative rates (up to 19 %) are reported for ILC than for other invasive cancers at mammography because ILC is often difficult to diagnose mammographically [46].

The most common clinical findings of ILC are palpable thickening and skin or nipple retraction [47]. When large, a firm palpable mass may become evident at clinical examination, often with the clinical examination findings being of greater concern for breast carcinoma than are the imaging findings. The mammogram often underestimates tumor size relative to the physical examination findings. ILC also has a propensity for metastatic spread to the peritoneum, retroperitoneum, and gynecologic organs. Therefore, metastatic ILC should be considered in women presenting with ascites, hydronephrosis, and/or pelvic masses [48].

10.5.9.2 Imaging

The sensitivity of mammography for the detection of ILC reportedly ranges between 57 and 80 %. The most frequent manifestation of ILC is architectural distortion with or without a central mass or a focal asymmetry. Calcifications are an uncommon feature of ILC. Unlike IDC, ILC is more frequently seen in only one view, most commonly in the craniocaudal view, which typically has better compression than the MLO view [49]. When ILC is large, the affected breast may appear to be decreasing in size on the mammogram, which has been termed the "shrinking breast" [50].

Sonography is a valuable adjunct to mammography, with reported sensitivities ranging from 68 to 98 % [51–54]. Sonography is superior to mammography in identifying multicentricity and multifocality and more accurately reflects the size of a mass than does mammography or clinical examination. The most common sonographic manifestation of ILC is an irregular or angular mass with hypoechoic and heterogeneous internal echoes, ill-defined or spiculated margins, and posterior acoustic shadowing, findings that are seen in 54–61 % of cases. Additional manifestations include circumscribed masses, focal shadowing without a discrete mass, as well as sonographically occult lesions. Although the US appearances of various subtypes of ILC overlap considerably, classic ILC tends to manifest as focal shadowing without a discrete mass, whereas pleomorphic type ILC is more typically seen as a shadowing mass. Signet ring, alveolar, and solid subtypes of ILC are more likely to manifest as a lobulated, well-circumscribed mass [46].

MR imaging is extremely useful for assessing the extent of the disease, with reported sensitivity of approximately 95 %. It is superior to mammography and ultrasound in estimating tumor size as well as identifying multifocal and multicentric disease. A meta-analysis by Mann et al. found that MR imaging was able to detect additional ipsilateral malignant findings not evident at mammography or US in 32 % of ILC patients. In addition, unexpected cancer in the contralateral breast was seen at MR imaging in 7 % of cases. MR imaging has been shown to affect clinical management in 50 % of patients with ILC, leading to changes in surgical management in

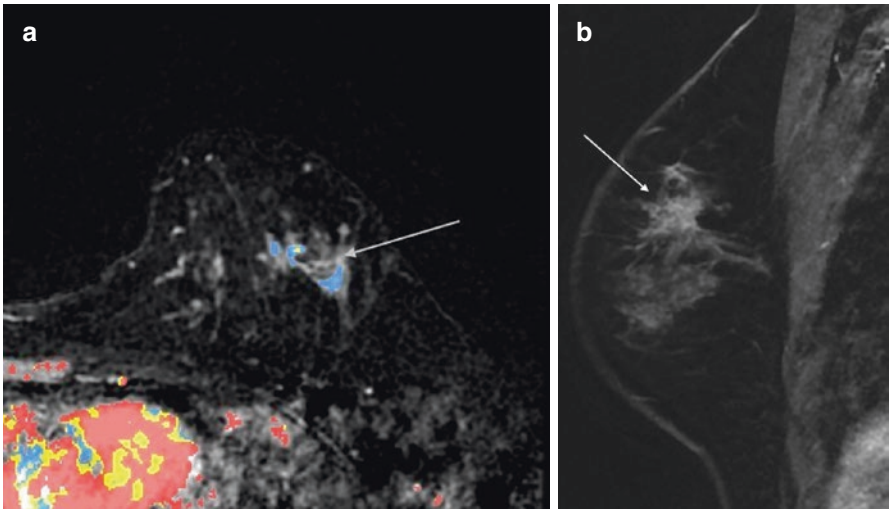

Fig. 10.12 (**a**) Axial post contrast color image demonstrates an area of nonmass enhancement with plateau kinetics (*arrow*). (**b**) Sagittal T1 post contrast image demonstrates nonmass enhancement (*arrow*). Biopsy revealed ILC at multiple sites

28 % of cases [46, 55–57]. In 39 % of women with ILC, MR imaging depicts more extensive disease than is suspected with conventional imaging [58]. On MR images, ILC may manifest as an enhancing solitary mass with irregular margins, multiple enhancing lesions, or only enhancing septations [46, 55–56, 58–59].

Additional manifestations include a dominant lesion surrounded by multiple small, enhancing foci, multiple small enhancing foci with interconnecting enhancing strands, architectural distortion, regional or focal heterogeneous NME, enhancing septa, and normal appearing breast parenchyma (Fig. 10.12). Interestingly, histopathologic findings suggest that the enhancing strands and septa correlate with tumor cells streaming within the breast stroma. Most ILC exhibit heterogeneous rather than homogeous enhancement, and some show poor enhancement [59]. ILC tends to demonstrate delayed maximum enhancement, with washout exhibited by only a minority of lesions [60]. Some ILCs may infiltrate and grow without significant angiogenesis and neovascularity, resulting in false negative MRI [60]. At MR spectroscopy, the tCho detection rate is also higher in IDC compared to ILC, which may be related to the infiltrating nature of ILC, resulting in fat contamination problem (from preserved background fat) in ILC [58].

A study assessing the impact of preoperative MRI on the re-excision rate in ILC found that patients who had an MRI had significantly lower re-excision rates compared with patients without preoperative MRI (9 % versus 27 %, respectively). This group also concluded that there was a trend towards a lower rate of final mastectomy in the ILC subgroup, although this finding did not attain significance [61]. Thus, women with ILC are among those most likely to benefit from the use of preoperative MRI for the assessment of extent of disease.

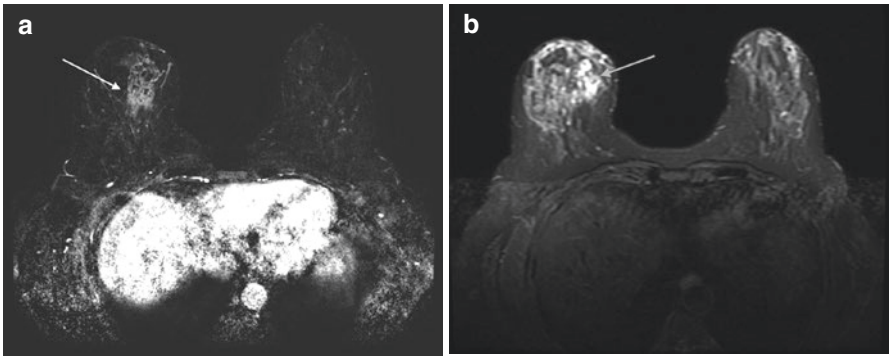

Fig. 10.13 Axial post contrast subtracted image demonstrates an irregular mass with heterogeneous enhancement (*white arrow*). T2 images demonstrate increased signal within the mass secondary to necrosis (*gray arrow*). Biopsy revealed metaplastic carcinoma

10.5.10 Metaplastic Carcinoma

10.5.10.1 Histology and Presentation

Metaplastic carcinoma is a mixed group of malignant neoplasms containing both glandular and nonglandular patterns with epithelial and/or mesenchymal components. Metaplastic carcinoma of the breast is a rare but aggressive type of breast cancer that has been recognized as a unique pathologic entity by the World Health Organization. Morphologically, it is characterized by the differentiation of neoplastic epithelium into squamous cells and/or mesenchymal-looking elements (squamous cells, spindle cells, cartilage or bone, etc.) [62]. It shares many similarities with invasive ductal carcinoma and benign lesions on mammography [62]. It is typically ER/PR/Her2 negative (triple negative).

Metaplastic carcinomas present primarily in women over 50 as a rapidly growing palpable mass [62]. Velasco et al. reported characteristics of 12 patients with metaplastic carcinoma. All masses demonstrated irregular shape and spiculated margins. T2 signal was variable but was greater that the surrounding tissue. T2 signals reported were homogeneous hypersignal(2/12), mottled hypersignal(9/12) and isointense (1/12). Contrast enhancement pattern was ringlike in 73 % and homogeneous in 27 % [63] (Fig. 10.13).

10.5.11 Phyllodes Tumors

10.5.11.1 Histology and Presentation

Phyllodes is a tumor of stromal origin. Phyllodes tumors account for fewer than 1 % of breast cancers and presents as rapidly enlarging palpable masses in middle-aged to older women [38]. Phyllodes tumors are generally benign. However 10 % of

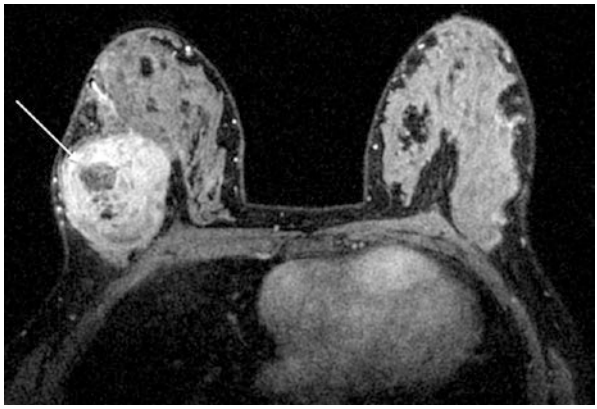

Fig. 10.14 Axial post contrast T1 image demonstrates an oval circumscribed mass with central areas of decreased enhancement (*arrow*). Biopsy revealed malignant phyllodes

phyllodes tumors are malignant. Phyllodes tumors are classified from low-grade to high-grade. Wide excision is indicated even for low-grade tumors, since a phyllodes tumor can be locally aggressive [38]. The risk of metastatic disease is very uncommon with phyllodes tumors. In the rare cases where the tumor does metastasize, these lesions spread hematogenously, most commonly to the lungs. A chest x-ray is useful in initial staging [38]. Sentinel node biopsy and axillary dissection is not helpful, since these tumors do not spread through the lymphatic system [38].

10.5.11.2 Imaging

On mammography, phyllodes tumors typically are seen as a large oval or round mass with circumscribed or ill-defined borders. Ultrasound often demonstrates an oval, hypoechoic mass similar to a fibroadenoma with multiple cystic spaces and mixed echogenicity [38]. MRI findings in a phyllodes tumor are similar to findings seen in a fibroadenoma. Findings include a well-marginated, oval or round mass with hypointense to isointense T1 signal and hyperintense T2 signal. Nonenhancing internal septations and variable enhancement curves from type 1 to type 3 may be present [64] (Fig. 10.14). High T2 signal in the surrounding breast tissue may be noted in a phyllodes. Cystic spaces with increased T2 signal may be present. Distinguishing a phyllodes from a fibroadenoma based on MRI is difficult [64].

10.6 Conclusion

In conclusion, recent understanding of the molecular nature of breast cancers has helped to explain certain imaging phenotypes seen on MRI. A variety of MR imaging characteristics can be seen with different histopathologic breast pathologies. Invasive ductal carcinoma presents most frequently as an irregular mass and often demonstrates Type 3 enhancement kinetics. Mucinous, papillary, adenoid cystic and

metaplastic carcinoma may demonstrate increased T2 signal. Delayed rim enhancement is a concerning finding seen in triple negative, adenoid cystic and medullary cancers. Lobular cancers can show minimal to no enhancement and present as masses, distortion, and non-mass enhancement. Tubular carcinomas display similar characteristics to invasive ductal carcinomas NOS, often appearing as an enhancing, spiculated mass. Attention to specific morphologic and kinetic characteristics can help in differentiating types of cancers. Recent MRI multiparametric developments such as diffusion and spectroscopy may be useful in identifying biologically significant invasive disease. Additionally, MRI may help in identifying axillary nodal involvement and in surgical planning.

References

1. Sung JS, Li J, Da Costa GD, Patil S, Van Zee KJ, Dershaw DD, et al. Preoperative breast MRI for early-stage breast cancer: effects on surgical and long-term outcomes. AJR Am J Roentgenol. 2014;202(6):1376–82.
2. Peters NH, Borel Rinkes IH, Zuithoff NP, Mali WP, Moons KG, Peeters PH. Meta-analysis of MR imaging in the diagnosis of breast lesions. Radiology. 2008;246(1):116–24. PMID:18024435.
3. Lehman CD, Isaacs C, Schnall MD, Pisano ED, Ascher SM, Weatherall PT, et al. Cancer yield of mammography, MR, and US in high-risk women: prospective multi-institution breast cancer screening study. Radiology. 2007;244(2):381–8.
4. Trop I, LeBlanc SM, David J, Lalonde L, Tran-Thanh D, Labelle M, et al. Molecular classification of infiltrating breast cancer: toward personalized therapy. Radiographics. 2014;34(5): 1178–95.
5. Uematsu T, Kasami M, Yuen S. Triple-negative breast cancer: correlation between MR imaging and pathologic findings. Radiology. 2009;250(3):638–47.
6. Molleran VM. MRI features of invasive disease. In: Molleran VM, Mahoney M, editors. Breast MRI. Philadelphia: Saunders Elsevier; 2013. p. 56.
7. Dogan BE, Gonzalez-Angulo AM, Gilcrease M, Dryden MJ, Yang WT. Multimodality imaging of triple receptor-negative tumors with mammography, ultrasound, and MRI. AJR Am J Roentgenol. 2010;194(4):1160–6.
8. Krizmanich-Conniff KM, Paramagul C, Patterson SK, Helvie MA, Roubidoux MA, Myles JD, et al. Triple receptor-negative breast cancer: imaging and clinical characteristics. AJR Am J Roentgenol. 2012;199(2):458–64.
9. Boo-Kyung H, Schnall MD, Orel S, Rosen M. Outcome of MRI-guided breast biopsy. AJR Am J Roentgenol. 2008;191(6):1798–804.
10. Morris EA, Comstock CE, Lee CH, et al. ACR BI-RADS® Magnetic Resonance Imaging. In: ACR BI-RADS® Atlas, Breast Imaging Reporting and Data System. Reston: American College of Radiology; 2013.
11. Tozaki M, Igarashi T, Fukuda K. Positive and negative predictive values of BI-RADS-MRI descriptors for focal breast masses. Magn Reson Med Sci. 2006;5(1):7–15.
12. Mahoney M, Gatsonis C, Hanna L, DeMartini WB, Lehman C. Positive predictive value of BI-RADS MR Imaging. Radiology. 2012;264(1):51–61.
13. Baltzer P, Benndorf M, Dietzel M, Gajda M, Runnebaum I, Kaiser W. False- positive findings at contrast-enhanced breast MRI: a BI-RADS descriptor study. AJR Am J Roentgenol. 2010;194(6):1658–63.
14. Menezes GL, Knuttel FM, Stehouwer BL, Pijnappel RM, Van Den Bosch MA. Magnetic resonance imaging in breast cancer: a literature review and future perspectives. World J Surg Oncol. 2014;5(2):61–70.

15. Kul S, Cansu A, Alhan E, Dinc H, Gunes G, Reis A. Contribution of diffusion -weighted imaging to dynamic contrast-enhanced MRI in the characterization of breast tumors. AJR Am J Roentgenol. 2011;196(1):210–7.
16. Ramírez de Molina AR, Gutiérrez R, Ramos MA, Silva JM, Bonilla F, Sanchez JJ, et al. Increased choline kinase activity in human breast carcinomas: clinical evidence for a potential novel antitumor strategy. Oncogene. 2002;21:4317–22.
17. Yeung DK, Yang WT, Tse GM, et al. Breast cancer: in vivo proton MR spectroscopy in the characterization of histopathologic subtypes and preliminary observations in axillary node metastases 1. Radiology. 2002;225(1):190–7.
18. Shin HJ, Baek HM, Cha JH, Kim HH. Evaluation of breast cancer using proton MR spectroscopy: total choline peak integral and signal-to-noise ratio as prognostic indicators. AJR Am J Roentgenol. 2012;198(5):W488–97.
19. Burstein HJ. The distinctive nature of HER2-positive breast cancers. N Engl J Med. 2005;353(16):1652–4.
20. Stefano R, Agostara B, Calabro M, Campisi I, Ravazzolo B, Traina A, et al. Expression levels and clinical-pathological correlations of HER2/neu in primary and metastatic human breast cancer. Ann N Y Acad Sci. 2004;1028(1):463–72.
21. Rabban J. A pathologist's overview of the pathology of breast disease. In: Kopans D, editor. Breast imaging. Philadelphia: Lippincott Williams and Wilkins; 2007. p. 62.
22. Bartella L, Dershaw D. Magnetic resonance imaging of invasive breast carcinoma. In: Morris E, Liberman L, editors. Breast MRI: diagnosis and intervention. New York: Springer Science & Business Media; 2005. p. 174–5.
23. Muttarak M, Lerttumnongtum P, Chaiwun B, Peh WC. Spectrum of papillary lesions of the breast: clinical, imaging, and pathologic correlation. AJR Am J Roentgenol. 2008;191(3): 700–7.
24. Riham E, Chong J, Kulkarni S, Goldberg F, Muradali D. Papillary lesions of the breast: MRI, ultrasound, and mammographic appearances. AJR Am J Roentgenol. 2012;198:264–71.
25. Molleran V. MRI features of invasive disease. In: Molleran V, Mahoney M, editors. Breast MRI. Philadelphia: Saunders Elsevier; 2013. p. 54–6.
26. Nassar H, Wallis T, Andea A, Dey J, Adsay V, Visscher D. Clinicopathologic analysis of invasive micropapillary differentiation in breast carcinoma. Mod Pathol. 2001;14(9):836–41.
27. Kuroda H, Sakamoto G, Ohnisi K, Itoyama S. Clinical and pathologic features of invasive micropapillary carcinoma. Breast Cancer. 2004;11(2):169–74.
28. Luna-More S, Gonzalez B, Acedo C, Rodrigo I, Luna C. Invasive micropapillary carcinoma of the breast. A new special type of invasive mammary carcinoma. Pathol Res Pract. 1994;190: 668–74.
29. Lim HS, Kuzmiak CM, Jeong SI, Choi YR, Kim JW, Lee JS, et al. Invasive micropapillary carcinoma of the breast: MR imaging findings. Korean J Radiol. 2013;14(4):551–8.
30. Tominaga J, Hama H, Kimura N, Takahashi S. MR imaging of medullary carcinoma of the breast. Eur J Radiol. 2009;70(3):525–9.
31. Bae SY, Choi MY, Cho DH, Lee JE, Nam SJ, Yang JH. Mucinous carcinoma of the breast in comparison with invasive ductal carcinoma: clinicopathologic characteristics and prognosis. J Breast Cancer. 2011;14(4):308–13.
32. Conant EF, Dillon RL, Palazzo J, Ehrlich SM, Feig SA. Imaging findings in mucin-containing carcinomas of the breast: correlation with pathologic features. AJR Am J Roentgenol. 1994; 163(4):821–4.
33. Lam WW, Chu WC, Tse GM, Ma TK. Sonographic appearance of mucinous carcinoma of the breast. AJR Am J Roentgenol. 2004;182(4):1069–74.
34. Kawashima M, Tamaki Y, Nonaka T, Higuchi K, Kimura M, Koida T, et al. MR imaging of mucinous carcinoma of the breast. AJR Am J Roentgenol. 2002;179(1):179–83.
35. Santamaría G, Velasco M, Bargalló X, Caparrós X, Farrús B, Fernández PL. Radiologic and pathologic findings in breast tumors with high signal intensity on T2-weighted MR images. Radiographics. 2010;30(2):533–48.

36. Woodhams R, Kakita S, Hata H, Iwabuchi K, Shigeaki U, Mountford C, et al. Diffusion-weighted imaging of mucinous carcinoma of the breast: evaluation of apparent diffusion coefficient and signal intensity in correlation with histologic findings. AJR Am J Roentgenol. 2009;193(1):260–6.
37. Monzawa S, Yokokawa M, Sakuma T, Takao S, Hirokaga K, Hanioka K, et al. Mucinous carcinoma of the breast: MRI features of pure and mixed forms with histopathologic correlation. AJR Am J Roentgenol. 2009;192(3):W125–31.
38. Harvey JA. Unusual breast cancers: useful clues to expanding the differential diagnosis. Radiology. 2007;242(3):683–94.
39. Sheppard DG, Whitman GJ, Fornage BD, Stelling CB, Huynh PT, Sahin AA. Tubular carcinoma of the breast: mammographic and sonographic features. AJR Am J Roentgenol. 2000;174(1):253–7.
40. Thompson K, Grabowski J, Saltzstein SL, Sadler GR, Blair SL. Adenoid cystic breast carcinoma: is axillary staging necessary in all cases? Results from the California cancer registry. Breast J. 2011;17(5):485–9.
41. Glazebrook KN, Reynolds C, Smith RL, Gimenez EI, Boughey JC. Adenoid cystic carcinoma of the breast. AJR Am J Roentgenol. 2010;194(5):1391–6.
42. Razek NMA, Hassan MAF, Fattah SA, Eshak SI. Dynamic MR-Mammography as the best method for diagnosis of invasive lobular breast carcinoma: A retrospective study. Egyptian J Radiol Nucl Med. 2013;44(2):405–9.
43. Berg WA, Gutierrez L, NessAiver MS, Carter WB, Bhargavan M, Lewis RS, et al. Diagnostic accuracy of mammography, clinical examination, US, and MR imaging in preoperative assessment of breast cancer. Radiology. 2004;233:830–49.
44. Yeatman TJ, Cantor AB, Smith TJ, Smith SK, Reintgen DS, Miller MS, et al. Tumor biology of infiltrating lobular carcinoma implications for management. Ann Surg. 1995;222:549–61.
45. Newstead GM, Baute PB, Toth HK. Invasive lobular and ductal carcinoma: mammographic findings and stage at diagnosis. Radiology. 1992;184(3):623–7.
46. Mann RM, Hoogeveen YL, Blickman JG, Boetes C. MRI compared to conventional diagnostic work-up in the detection and evaluation of invasive lobular carcinoma of the breast: a review of existing literature. Breast Cancer Res Treat. 2008;107(1):1–14.
47. Le Gal M, Ollivier L, Asselain B, Meunier M, Laurent M, Vielh P, et al. Mammographic features of 455 invasive lobular carcinomas. Radiology. 1992 Dec;185(3):705–8.
48. Winston CB, Hadar O, Teitcher JB, Caravelli JF, Sklarin NT, Panicek DM, et al. Metastatic lobular carcinoma of the breast: patterns of spread in the chest, abdomen, and pelvis on CT. AJR Am J Roentgenol. 2000;175(3):795–800.
49. Porter AJ, Evans EB, Foxcroft LM, Simpson PT, Lakhani SR. Mammographic and ultrasound features of invasive lobular carcinoma of the breast. J Med Imaging Radiat Oncol. 2014;58(1):1–10.
50. Harvey JA, Fechner RE, Moore MM. Apparent ipsilateral decrease in breast size on mammography: a sign of infiltrating lobular carcinoma. Radiology. 2000;214(3):883–9.
51. Butler RS, Venta LA, Wiley EL, Ellis RL, Dempsey PJ, Rubin E. Sonographic evaluation of infiltrating lobular carcinoma. AJR Am J Roentgenol. 1999;172(2):325–30.
52. Helvie MA, Paramagul C, Oberman HA, Adler DD. Invasive lobular carcinoma: imaging features and clinical detection. Invest Radiol. 1993;28(3):202–7.
53. Paramagul CP, Helvie MA, Adler DD. Invasive lobular carcinoma: sonographic appearance and role of sonography in improving diagnostic sensitivity. Radiology. 1995;195(1):231–4.
54. Evans WP, Warren Burhenne LJ, Laurie L, O'Shaughnessy KF, Castellino RA. Invasive lobular carcinoma of the breast: mammographic characteristics and computer-aided detection. Radiology. 2002;225(1):182–9.
55. Schelfout K, Van Goethem M, Kersschot E, Verslegers I, Biltjes I, Leyman P, et al. Preoperative breast MRI in patients with invasive lobular breast cancer. Eur Radiol. 2004;14(7):1209–16.
56. Munot K, Dall B, Achuthan R, Parkin G, Lane S, Horgan K. Role of magnetic resonance imaging in the diagnosis and single-stage surgical resection of invasive lobular carcinoma of the breast. Br J Surg. 2002;89(10):1296–301.

57. Del Frate C, Borghese L, Cedolini C, Bestagno A, Puglisi F, Isola M, et al. Imaging in the diagnosis and single-stage surgical resection of invasive lobular carcinoma Role of pre-surgical breast MRI in the management of invasive breast carcinoma. Breast. 2007;16(5):469–81.
58. Weinstein SP, Orel SG, Heller R, Reyonalds C, Czerniecki B, Solin LJ, et al. MR imaging of the breast in patients with invasive lobular carcinoma. Am J Roentgenol. 2001;176(2): 399–406.
59. Qayyum A, Birdwell RL, Daniel BL, Nowels KW, Jeffrey SS, TA A, et al. MR imaging features of infiltrating lobular carcinoma of the breast: histopathologic correlation. AJR Am J Roentgenol. 2002;178(5):1227–32.
60. Yeh ED, Slanetz PJ, Edmister WB, Talele A, Monticciolo D, Kopans DB. Invasive lobular carcinoma: spectrum of enhancement and morphology on magnetic resonance imaging. Breast J. 2003;9(1):13–8.
61. Mann RM, Loo CE, Wobbes T, Bult P, Barentsz JO, Gilhuijs KG, et al. The impact of preoperative breast MRI on the re-excision rate in invasive lobular carcinoma of the breast. Breast Cancer Res Treat. 2010;119(2):415–22.
62. McKinnon E, Xiao P. Metaplastic carcinoma of the breast. Arch Pathol Lab Med. 2015;139(6): 819–22.
63. Velasco M, Santamaría G, Ganau S, Farrús B, Zanón G, Romagosa C, et al. MRI of metaplastic carcinoma of the breast. AJR Am J Roentgenol. 2005;184(4):1274–8.
64. Wurdinger S, Herzog AB, Fischer DR, Marx C, Raabe G, Schneider A, et al. Differentiation of phyllodes breast tumors from fibroadenomas on MRI. AJR Am J Roentgenol. 2005;185(5): 1317–21.